

- obtain the scattered intensity  $I(\mathbf{q})$ , the displacement  $u(r)$  appears in the argument of an exponential and thus enters  $I(\mathbf{q})$  in a nonlinear way. Thus, with sinusoidal undulation, even though  $u(r)$  has only the single (fundamental) harmonic, multiple diffraction orders appear versus  $m$  for  $s = 1, 2$ .
45. The  $d_m$  values quoted here are for fresh samples in capillaries.  $d_m$  was found to increase in time with x-ray exposure and aging at B7 temperatures (up to  $d_m \sim 600$  Å in MHOBOW). This effect was particularly noticeable in freely suspended film and freeze fracture experiments, where there is more exposure to air during observation and preparation, respectively.
  46. J. A. Zasadzinski, *J. Phys.* **51**, 747 (1990).
  47. T. Gulik-Krzywicki, M. J. Costello, *J. Microsc.* **112**, 103 (1997).
  48. Several recent papers use evidence for polarization along the layer normal in B7 phases to argue that they are simply lamellar with triclinic local layer symmetry (9, 49). However, the phases in question are shown here to be undulated and polarization modulated so that the claim of triclinic behavior in a lamellar smectic may not be justified. In fact, a PM phase is triclinic essentially everywhere (wherever there is nonzero layer curvature). It may be that local triclinic symmetry actually drives the PM, but there is no evidence for this at present.
  49. A. Jákli, D. Krücker, H. Sawade, G. Heppke, *Phys. Rev. Lett.* **86**, 5715 (2001).
  50. It is not understood why  $d_m$  is larger in films than in bulk, but this may be due either to surface tension, which provides an additional elastic resistance to undulation, or due to the high surface-to-volume ratio of the films, which enhances hydrolysis and impurity buildup.
  51. S. W. Choi *et al.*, *Mol. Cryst. Liq. Cryst.* **328**, 185 (1999).
  52. M. Nakata, N. Chattham, N. A. Clark, H. Takezoe, unpublished data.
  53. C. Y. Young, R. Pindak, N. A. Clark, R. B. Meyer, *Phys. Rev. Lett.* **40**, 773 (1978).
  54. The B7 materials strongly favor formation of freely suspended filaments (12, 16) rather than films, a consequence of their 2D lattice structure, but it was possible to obtain 1- to 10-layer-thick MHOBOW and 10OAM5AMO10 films at high  $T$  in the B7 phase by either pulling the film very slowly ( $\sim 20$   $\mu\text{m/s}$ ) or by applying an ac field ( $\sim 5$  V/mm) parallel to the film plane during the pulling. An initially thin spot will expand in area over a large fraction of the film after several hours.
  55. R. Pindak, C. Y. Young, R. B. Meyer, N. A. Clark, *Phys. Rev. Lett.* **45**, 1193 (1980).
  56. A. Hauser, A. Schamalfuss, Kresse, *Liq. Cryst.* **27**, 629 (2000).
  57. Several B7 phases have been previously identified as SmCP<sub>A</sub> on the basis of antiferroelectric properties, including absence of second-order nonlinear optical susceptibility. We contend that the underlying structure is actually SmC<sub>s</sub>P<sub>F</sub> and that the antiferroelectricity is that of the PM stripe pattern.
  58. R. Stannarius, C. Langer, W. Weissflog, *Phys. Rev. E* **66**, 031709 (2002).
  59. Because the field-induced PM/UL-to-SmCP transition is an equilibrium energetic effect, the modulation should in principle return once the field is removed. However, it did not do so spontaneously in any of the experiments reported here or in (6). This is likely due to the fact that in order to reach the threshold field, the LC was only 1 to 5  $\mu\text{m}$  thick, and because the layer structure shrinkage upon PM expulsion was locked in by the surfaces, an effect similar to the irreversible elimination of the chevron structure in SmCs by field application. The PM/UL-to-SmCP transition in CITRO could be reversed by waveform selection (square wave: PM/UL-to-SmCP; triangle wave: SmCP -to- PM/UL) (10).
  60. If  $p$  is the pitch of a helical winding of  $\mathbf{m}(x)$  along a filament, then at radius  $\rho$  from the filament core we have  $\alpha(\rho) = \rho(2\pi/p)$ . Thus, if the pitch is independent of  $\rho$ , then the orientation of  $\mathbf{m}$  also winds helically versus  $\rho$  at a given  $x$  and the PM lattice must have TGBs.
  61. C. R. Safinya, K. S. Liang, W. A. Varady, N. A. Clark, G. Andersson, *Phys. Rev. Lett.* **53**, 1172 (1984).
  62. C. R. Safinya, N. A. Clark, K. S. Liang, W. A. Varady, L. Y. Chiang, *Mol. Cryst. Liq. Cryst.* **123**, 205 (1985).
  63. The elastic constant  $C$  of the PM lattice is comparable to its elastic energy density  $C \sim K/d_m^2 \sim 10^4$  J/m<sup>3</sup> (see calculation of  $E_{\text{th}}$ ), about four orders of magnitude smaller than typical smectic layer compression moduli. Thus, the typical fluid smectic focal conic organization of layers is maintained.
  64. The winding of the 2D PM lattice on a filament of fixed cross-sectional layer structure is maintained topologically by the number of undulation periods around the filament. However, the PM lattice must have dislocations because of the curvature of the smectic layers (Fig. 7, B and C).
  65. J. Szydłowska *et al.*, *Phys. Rev. E* **67**, 031702 (2003).
  66. The B1 lattice structure shown in Fig. 1H is one of many possibilities for alternation of polarization and tilt orientation, which also include PM in the absence of tilt. Thus, the homochiral, synpolar case (e.g., all stripe polarizations toward the reader and in magenta) would necessarily have an oblique 2D lattice, which has been found in some B1s, e.g., W1044.
  67. The polarization is sketched as uniform in the B1 phase in (53) and the B1rev phase in (69), but in fact must be splayed, e.g., as in Fig. 1H.
  68. W. L. McMillan, *Phys. Rev. A* **4**, 1238 (1971).
  69. W1044 has an oblique 2D reciprocal lattice characterized by strong  $[s, m] = [1, 1]$  and  $[1, -1]$  reflections, with complete absence of the  $s = 1, m$  even reflections, indicative of an interdigitated real lattice. The real lattice is as in Fig. 1H but oblique, possibly due to a uniform rather than alternating molecular tilt orientation (43).
  70. M. Brunet, L. Navailles, N. A. Clark, *Eur. Phys. J. E* **7**, 5 (2002).
  71. A. Eremin, S. Diele, G. Pelzl, W. Weissflog, *Phys. Rev. E* **67**, 020702(R) (2003).
  72. J. Ortega, C. L. Folcia, J. Etxebarria, N. Gimeno, M. B. Ros, *Phys. Rev. E* **68**, 011707 (2003).
  73. B. N. Thomas, N. A. Clark, *Phys. Rev. E* **59**, 3040 (1999).
  74. S. Pakhomov *et al.*, *Proc. Natl. Acad. Sci. U.S.A.* **100**, 3040 (2003).
  75. This work was supported by NSF grant DMR-0072989, NSF Materials Research Science and Engineering Centers grants 0213918 (University of Colorado) and 0080034 (University of California, Santa Barbara), and NASA grant NAG3-2457. Research was carried out in part at the National Synchrotron Light Source, supported by U.S. Department of Energy, Divisions of Materials and Chemical Sciences.

## Supporting Online Material

www.sciencemag.org/cgi/content/full/301/5637/1204/DC1

Figs. S1 to S3

26 March 2003; accepted 4 August 2003

## Major Ecological Transitions in Wild Sunflowers Facilitated by Hybridization

Loren H. Rieseberg,<sup>1\*</sup> Olivier Raymond,<sup>2</sup> David M. Rosenthal,<sup>3</sup> Zhao Lai,<sup>1</sup> Kevin Livingstone,<sup>1</sup> Takuya Nakazato,<sup>1</sup> Jennifer L. Durphy,<sup>1</sup> Andrea E. Schwarzbach,<sup>4</sup> Lisa A. Donovan,<sup>3</sup> Christian Lexer<sup>1</sup>

Hybridization is frequent in many organismal groups, but its role in adaptation is poorly understood. In sunflowers, species found in the most extreme habitats are ancient hybrids, and new gene combinations generated by hybridization are speculated to have contributed to ecological divergence. This possibility was tested through phenotypic and genomic comparisons of ancient and synthetic hybrids. Most trait differences in ancient hybrids could be recreated by complementary gene action in synthetic hybrids and were favored by selection. The same combinations of parental chromosomal segments required to generate extreme phenotypes in synthetic hybrids also occurred in ancient hybrids. Thus, hybridization facilitated ecological divergence in sunflowers.

The role of hybridization in evolution has been debated for more than a century. Two highly polarized viewpoints have emerged. At one extreme, hybridization is considered to be a potent evolutionary force that creates opportunities for adaptive evolution and speciation (1, 2). In this view, the increased genetic variation and new gene

combinations resulting from hybridization promote the development and acquisition of novel adaptations. The contrasting position accords little evolutionary importance to hybridization (aside from allopolyploidy), viewing it as a primarily local phenomenon with only transient effects—a kind of “evolutionary noise” (3–5). Unfortunately, definitive support for either viewpoint is lacking. Although footprints of past hybridization are often detected by molecular phylogenetic studies (6), their presence does not indicate that the hybridization was adaptive. Likewise, the documentation of fit hybrids in contemporary hybrid zones (2) is not proof of an adaptive role for hybridization, because fit

<sup>1</sup>Department of Biology, Indiana University, Bloomington, IN 47405, USA. <sup>2</sup>Laboratoire de Biologie Moléculaire et Phytochimie, Université Claude Bernard Lyon 1, F-69622 Villeurbanne, France. <sup>3</sup>Department of Plant Biology, University of Georgia, Athens, GA 30602, USA. <sup>4</sup>Department of Biological Sciences, Kent State University, Kent, OH 44242, USA.

\*To whom correspondence should be addressed. E-mail: lriesebe@indiana.edu

RESEARCH ARTICLES

hybrid genotypes may be transitory as a result of recombination (7).

One means by which fit hybrid genotypes may become established is through diploid hybrid speciation (8, 9). In this process, a reproductive barrier arises in a new hybrid lineage, which protects it from gene flow with its parental species or other hybrid genotypes. Models of diploid hybrid speciation suggest that reproductive isola-

tion may arise through rapid chromosomal repatterning, ecological divergence, and/or spatial separation (8, 10). Ecological divergence may be of particular importance to the process, because computer simulations indicate that hybrid speciation is unlikely in the absence of niche separation (10, 11), and all documented examples of diploid hybrid species are divergent ecologically from their parental species (12, 13). Indeed,

hybrid species often occur in habitats more extreme than those of any congener (14). Evidence that hybridization has played a key role in adaptation to these novel or extreme habitats would support the hypothesis that hybridization can be an important creative force in evolution.

Here, we ask whether hybridization has facilitated major ecological transitions in annual sunflowers of the genus *Helianthus*, a group

**Table 1.** Comparisons of morphological, life history, and physiological traits among *H. annuus* and *H. petiolaris* and their three hybrid derivative species: *H. anomalus*, *H. deserticola*, and *H. paradoxus*. Only traits that map to linkage groups 1 and 10 are shown (see table S1 for comparisons of all 40 traits). Traits that significantly differ between the two parental species, *H. annuus* and *H. petiolaris*, are indicated with an asterisk. For the ancient hybrid species, traits that significantly exceed both parental trait values are referred to as "extreme." Those that are significantly different but intermediate between the parental species are referred to as "intermediate." Traits that do not differ significantly from one or both parental species are designated ANN-like, PET-like, or ANN/PET-like. Trait abbreviations and units of measure are as

follows: DISKDIA, disk diameter (mm); LFAREA, leaf area (cm<sup>2</sup>); LFSHAP, leaf shape (length/width ratio); LFWIDTH, leaf width (mm); LIGLGTH, ligule length (mm); LIGNUM, number of ligules or ray flowers; PHYLGTH, phyllary length (mm); PHYNUM, phyllary number; RTL96, root length after 96 hours (mm); SEEDW, initial seed weight (mg); STEM DIA, stem diameter at 2 cm above the ground (mm); BUDDAY, days until budding; FLBIO, flower biomass (g); FLODAY, days until first floret; RGR, relative growth rate (cm/day); B, leaf boron concentration (ppm); Ca, leaf calcium concentration (ppm); K, leaf potassium concentration (ppm); Mg, leaf magnesium concentration (ppm); Mn, leaf manganese concentration (ppm); SLA, specific leaf area (cm<sup>2</sup>/g). Means ± SD are shown for the two parental species.

Trait	<i>H. annuus</i> (ANN)	<i>H. petiolaris</i> (PET)	<i>H. anomalus</i> (ANO)	<i>H. deserticola</i> (DES)	<i>H. paradoxus</i> (PAR)
<i>Morphological traits</i>					
DISKDIA*	27.48 ± 5.14	16.24 ± 2.40	13.19 Extreme	12.04 Extreme	15.24 PET-like
LFAREA*	63.30 ± 36.79	24.97 ± 9.48	19.25 Extreme	20.21 Extreme	92.18 Extreme
LFSHAP*	1.71 ± 0.27	2.35 ± 0.58	4.47 Extreme	3.63 Extreme	2.79 PET-like
LFWIDTH*	75.9 ± 2.4	42.1 ± 10.9	27.4 Extreme	28.4 Extreme	70.8 ANN-like
LIGLGTH*	34.7 ± 6.0	28.28 ± 4.30	29.65 PET-like	25.68 PET-like	26.25 PET-like
LIGNUM*	18.32 ± 3.06	11.59 ± 2.15	10.63 Extreme	10.25 Extreme	14.70 Intermediate
PHYLGTH*	21.3 ± 3.9	13.0 ± 2.2	23.6 Extreme	15.1 PET-like	11.7 PET-like
PHYNUM*	27.00 ± 4.61	18.82 ± 2.40	17.19 PET-like	16.88 Extreme	18.60 PET-like
RTL96	13.2 ± 6.0	6.4 ± 3.9	13.2 ANN-like	8.6 PET-like	12.2 ANN-like
SEEDW	5.64 ± 0.37	1.71 ± 0.32	7.39 Extreme	3.11 Intermediate	4.24 Intermediate
STEM DIA	14.54 ± 1.63	7.55 ± 1.16	6.02 Extreme	7.74 PET-like	11.15 Intermediate
<i>Life history traits</i>					
BUDDAY*	37.85 ± 11.11	34.35 ± 6.91	45.31 Extreme	29.50 Extreme	100.06 Extreme
FLBIO*	55.7 ± 10.4	10.0 ± 4.8	6.0 PET-like	4.8 PET-like	11.8 PET-like
FLODAY*	59.35 ± 13.94	48.71 ± 7.24	60.19 ANN-like	42.50 Extreme	106.00 Extreme
RGR	2.56 ± 0.40	2.37 ± 0.50	2.36 PET-like	2.34 PET-like	1.19 Extreme
<i>Physiological traits</i>					
B*	66.04 ± 19.18	66.54 ± 16.93	61.86 ANN/PET-like	32.10 Extreme	39.81 Extreme
Ca	16,927.34 ± 7064.30	19,685.13 ± 7358.02	13,436.70 ANN/PET-like	16,843.16 ANN/PET-like	22,338.20 ANN/PET-like
K*	49,226.90 ± 6831.37	61,708.53 ± 5885.27	44,451.29 Extreme	49,298.71 ANN-like	38,310.09 Extreme
Mg*	3283.18 ± 582.83	4212.85 ± 542.28	3455.07 Intermediate	4271.48 PET-like	5698.12 Extreme
Mn	196.69 ± 32.79	216.42 ± 61.76	215.35 ANN/PET-like	189.62 ANN/PET-like	354.12 Extreme
SLA*	207.88 ± 50.55	320.17 ± 72.87	240.53 Intermediate	268.67 Intermediate	241.85 Intermediate

Downloaded from www.sciencemag.org on January 4, 2008

that is ideal for addressing this question. Molecular phylogenetic evidence indicates that three of the 11 species in this group (*H. anomalus*, *H. deserticola*, and *H. paradoxus*) are stabilized diploid hybrid derivatives of two widespread species, *H. annuus* and *H. petiolaris* (14). The hybrid species appear to have been derived independently from the parental species and are found in the most extreme habitats of any *Helianthus* species: *H. anomalus* occurs on sand dunes in Utah and northern Arizona, USA; *H. deserticola* inhabits dry, sandy soils on the desert floor in Nevada, Utah, and Arizona; and *H. paradoxus* is restricted to a handful of brackish salt marshes in west Texas and New Mexico. In contrast, the two parental species are broadly distributed throughout the central and western United States and occur in less extreme environments. *Helianthus annuus* inhabits mesic, clay-based soils that are wet in the spring but may dry out later in the summer. *Helianthus petiolaris* occurs in sandier soils with less vegetation cover. Finally, microsatellite divergence of the three hybrid species from their parents suggests that they originated between 60,000 and 200,000 years before the present (15–17). Thus, they arose recently enough to make par-

tial experimental replication feasible (18, 19), yet are ancient enough to exclude anthropogenic influences in their origin.

We have used several approaches to study the role of hybridization in ecological adaptation and speciation in this group, including detailed phenotypic comparisons of synthetic and natural sunflower hybrids, selection experiments in natural sites, quantitative trait locus (QTL) analyses of synthetic hybrids, and comparisons of genomic composition between the synthetic and ancient hybrids. We ask the following questions: (i) Can the extreme traits displayed by the ancient hybrid species be experimentally generated by hybridizing the parental species? (ii) Are these phenotypes favored in the natural habitats of the hybrid species? (iii) What is the genetic basis of the extreme trait values? (iv) Do genetic correlations facilitate or impede ecological divergence? (v) Can the genomic composition of the ancient hybrid species be predicted from the QTL analysis of synthetic hybrids? That is, do the ancient hybrid species have the predicted combination of parental chromosomal segments for producing their extreme phenotypes?

**Can trait differences in ancient hybrids be recreated in synthetic hybrids?**

We first asked whether traits that differentiate the ancient hybrid species from their parents (20) could be recreated by hybridizing contemporary populations of the parental species. This question was addressed by propagating 20 individuals of each of the five species plus 400 BC<sub>2</sub> hybrids of *H. annuus* × *H. petiolaris* in the University of Georgia greenhouses (21). All plants that survived to maturity were measured for 22 morphological, 6 life history, and 12 physiological traits (Table 1) (table S1).

When compared to the parental species, *H. anomalus* differed significantly for 20 of the 40 traits (Table 1) (table S1). Of these 20 traits, 13 significantly exceeded the parental trait values and seven were intermediate. For *H. deserticola*, 11 traits were extreme relative to the parental species and three were intermediate. *Helianthus paradoxus* was the most divergent of the three hybrid species, with 15 extreme and eight intermediate traits.

Intermediate trait values are most easily accounted for in hybrid species because hybrids combine alleles from both parental spe-

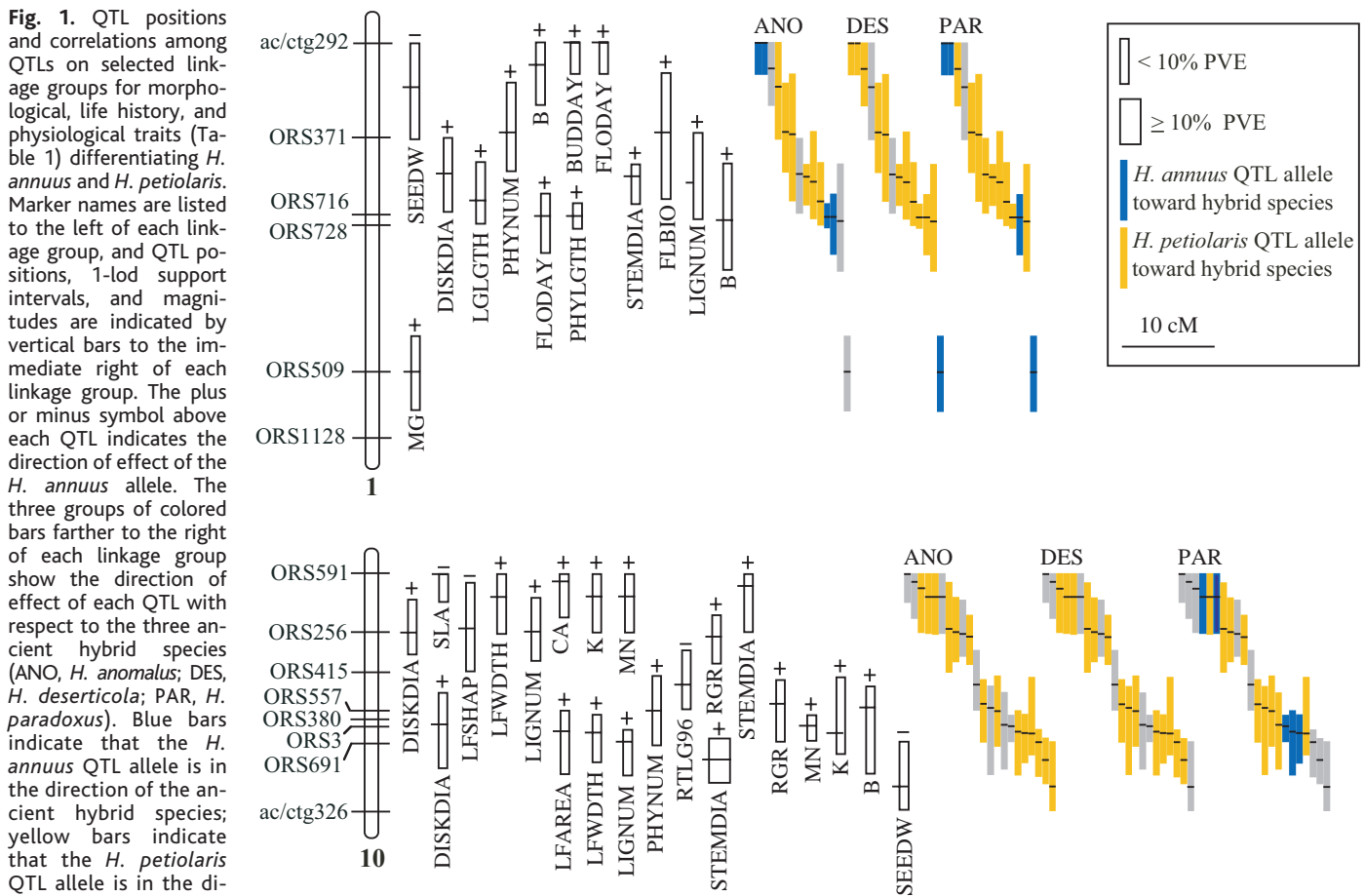


**Fig. 1.** QTL positions and correlations among QTLs on selected linkage groups for morphological, life history, and physiological traits (Table 1) differentiating *H. annuus* and *H. petiolaris*. Marker names are listed to the left of each linkage group, and QTL positions, 1-*lod* support intervals, and magnitudes are indicated by vertical bars to the immediate right of each linkage group. The plus or minus symbol above each QTL indicates the direction of effect of the *H. annuus* allele. The three groups of colored bars farther to the right of each linkage group show the direction of effect of each QTL with respect to the three ancient hybrid species (ANO, *H. anomalus*; DES, *H. deserticola*; PAR, *H. paradoxus*). Blue bars indicate that the *H. annuus* QTL allele is in the direction of the ancient hybrid species; yellow bars indicate that the *H. petiolaris* QTL allele is in the direction of the ancient hybrid. Gray bars indicate that the hybrid species is intermediate for the trait or cannot be differentiated from either parental species. Overlapping bars that are mostly the same color (excluding the

gray bars) indicate that genetic correlations are favorable for producing the multitrait phenotype of the corresponding ancient hybrid species.

cies. Indeed, the full range of intermediate values were recovered for all traits in the synthetic BC<sub>2</sub> hybrids (table S1). However, extreme phenotypic values are frequently reported in segregating hybrids as well, a phenomenon referred to as transgressive segregation. A recent survey of 171 studies of segregating hybrids revealed that 536 (43.6%) of 1229 traits examined were transgressive (22). An even higher proportion of extreme traits was observed in the present study. Twenty-five (62.5%) or 27 (67.5%) of the 40 traits assayed in the BC<sub>2</sub> hybrids were transgressive, depending on whether the observed number of extreme phenotypes was compared to expectations for two versus three standard deviations, respectively (table S1). These are very high percentages for wild, outcrossing species (22).

There was not a perfect match, however, between the extreme traits observed in the three ancient hybrid species and the presence or direction of transgression in the BC<sub>2</sub> population. In some instances, the lack of significant transgression appears to be a statistical artifact of high levels of phenotypic variation in one of the parental species, but for other traits the range of phenotypic variation in the BC<sub>2</sub> is truly narrow. Thus, a more relevant measure of the possible contribution of hybridization to phenotypic divergence is the proportion of extreme traits that are within the range of variation found in the BC<sub>2</sub> population. For *H. anomalus*, 11 of 13 (84.6%) extreme traits were within the range of the BC<sub>2</sub> population and thus could be accounted for by hybridization (table S1). All 11 extreme traits (100%) in *H. deserticola* were within the range of phenotypic variation observed in the BC<sub>2</sub>, and 10 of 15 (66.7%) extreme traits in *H. paradoxus* could be accounted for by hybridization (table S1). Traits beyond the range of the BC<sub>2</sub> population might be transgressive in a reciprocal backcross population. Alternatively, they may have arisen through mutational divergence rather than hybridization. Either way, it is clear that the majority of extreme traits observed in the ancient hybrid species could have been generated through hybridization.

**Are the extreme phenotypes adaptive?**

Although the three ancient hybrid species are phenotypically divergent with respect to their parental species, the trait differences do not necessarily represent adaptations to the habitats in which they occur. They could, for example, have diverged through drift or as a by-product of adaptive developmental changes (23). There are two kinds of evidence, however, that suggest that many of the trait differences are adaptive.

First, the three hybrid species have suites of traits that are commonly observed in unrelated taxa found in the same habitats. For example, *H. anomalus*, like other sand dune endemics, has large seeds, rapid root growth, and succulent leaves (Table 1) (table S1). Large seeds reduce the probability of burial by moving sand, rapid root growth helps tap into water reserves, and succulent leaves reduce water loss in arid environments (24). *Helianthus deserticola* has many classic features of a desert annual, including rapid flowering, small narrow leaves, and reduced boron uptake (Table 1) (table S1). Rapid flowering ensures reproduction after heavy seasonal rain, the small narrow leaves decrease water loss and avoid fatal overheating (25), and reduced boron uptake may increase boron toxicity tolerance in low-rainfall regions. Like many other salt-loving species (halophytes), *H. paradoxus* reduces the toxic effects of sodium and other mineral ions through active exclusion (26), internal sequestration, and increased leaf succulence (27).

Second, we have conducted a series of experiments in parallel to those reported here, in which BC<sub>2</sub>, parental, and hybrid species individuals were transplanted into the habitat of each of the ancient hybrid species. The results from these experiments have been fully analyzed only for the *H. paradoxus* habitat (26), but they are illustrative of preliminary findings from the *H. anomalus* and *H. deserticola* sites. As predicted, leaf succulence and mineral ion uptake are under strong directional selection in the *H. paradoxus* habitat, and the strength of selection for QTLs underlying these traits (the selection coefficient, *s*, rang-

es from 0.08 to 0.13) is strong enough to account for the origin of *H. paradoxus* in parapatry with its parental species (26). Also, QTLs from both parental species were significantly positively selected in the *H. paradoxus* habitat, as required for models of diploid hybrid speciation (10).

**What is the mode of gene action responsible for transgression?**

To determine how extreme phenotypes are generated through hybridization, we genotyped 384 BC<sub>2</sub> plants of *H. annuus* × *H. petiolaris* for 96 molecular markers known to cover most of the sunflower genome (21). The genomic location, percentage of variance explained (PVE), and additive effects of QTLs underlying the 40 traits scored in the previous experiment were estimated with composite interval mapping (21). In addition, all pairs of marker loci were tested for interaction effects or epistasis (21).

We detected 185 QTLs for the 40 traits (Fig. 1) (fig. S1 and table S2). QTL effects were modest in magnitude, ranging from 4 to 17% PVE. However, it is the directionality of QTL effects that is most relevant to the issue of transgressive segregation. More than 39% of QTL effects were in the opposite direction of species differences, and 34 of the 40 traits analyzed had at least one opposing QTL (fig. S1 and table S2). That is, for these QTLs, the *H. annuus* allele produced a more *H. petiolaris*-like phenotype, and vice versa.

The presence of QTLs with opposing effects provides a simple explanation for transgressive segregation: Segregating hybrids can combine plus alleles or minus alleles from both parents, thereby generating extreme phenotypes (Table 2). This “complementary gene action” model accounts for most of the transgressive phenotypes observed in the *H. annuus* × *H. petiolaris* BC<sub>2</sub> population (table S2). All but five of the transgressive traits had complementary QTLs. Of the five traits that lacked opposing QTLs, three had a single detected QTL, and thus the complementary gene model could not be tested. For the two remaining traits (LIGNUM and SLA), putative antagonistic QTLs were detected that barely fell beneath the significance threshold. On the other hand, some traits had complementary QTLs but did not display significant phenotypic transgression. This could be due to the limited sample size of the BC<sub>2</sub> population or to high phenotypic variance in the parental species.

Although most transgressive phenotypes can be accounted for by complementary genes, epistatic interactions appear to contribute as well. Significant epistasis was observed for 18 traits, 14 of which showed significant transgression (tables S1 and S3). These observations are broadly consis-

**Table 2.** Hypothetical example of transgressive segregation due to the complementary action of genes with additive effects.

QTLs	Phenotypic values			
	Species A (AA genotype)	Species B (BB genotype)	Transgressive F <sub>2</sub>	Transgressive F <sub>2</sub>
1	+1	-1	+1 (AA)	-1 (BB)
2	+1	-1	+1 (AA)	-1 (BB)
3	+1	-1	+1 (AA)	-1 (BB)
4	-1	+1	+1 (BB)	-1 (AA)
5	-1	+1	+1 (BB)	-1 (AA)
Total	+1	-1	+5	-5

tent with evidence from studies of cultivated plants, in which complementary gene action is the primary cause of transgressive segregation, with less frequent contributions from epistasis and overdominance (22, 28).

**Do genetic correlations facilitate or impede ecological divergence?** The phenotypic comparisons and QTL experiments described above indicate that most trait differences in the ancient hybrid species can be recovered by hybridizing their parental species. To generate the complex, multitrait phenotype of a hybrid species, however, it is necessary to combine all trait differences into a single individual. This will only be possible if closely linked or pleiotropic QTLs have effects that are in the same direction with respect to the hybrid species phenotype. Thus, for each of the hybrid species, we asked whether correlations among closely linked or pleiotropic QTLs were suitable for producing their phenotype (21). This was accomplished by testing whether the positions [i.e., 1-*lod* (logarithm of the odds ratio for linkage = 1) support intervals] of QTLs with effects in the same direction with respect to a given hybrid species phenotype overlapped more frequently than would be expected by chance (Fig. 1) (fig. S1). Congruence in the direction of QTL effects was measured with the  $\phi$  coefficient of association, a standard measure of association that can vary from  $-1$  to  $1$  (29).

Overlapping QTLs most often had effects in the same direction with respect to the phenotypes of the ancient hybrid species (Fig. 1) (fig. S1). The  $\phi$  coefficient of association was  $0.32$  ( $N = 256$ ,  $P < 0.001$ ) for *H. paradoxus*,  $0.47$  ( $N = 256$ ,  $P < 0.001$ ) for *H. anomalus*, and  $0.53$  ( $N = 256$ ,  $P < 0.001$ ) for *H. deserticola*. Note that these are conservative estimates of congruence levels, because the 1-*lod* support intervals for some QTLs were large (Fig. 1) (fig. S1 and table S2). Incongruence of QTL directions for QTLs within 2 cM of each other are infrequent; only 4, 5, and 10 such instances of incongruence were observed for *H. anomalus*, *H. deserticola*, and *H. paradoxus*, respectively.

These results indicate that genetic correlations likely facilitated the origin of the three ancient hybrid species and the acquisition of their multitrait phenotypes, particularly for *H. anomalus* and *H. deserticola*. It is noteworthy that both species carry multiple chloroplast DNA haplotypes from their parental species (15, 16), which suggests that they may be multiply derived in nature. In contrast, less frequent positive genetic correlations make it difficult to recreate the multitrait phenotype of *H. paradoxus*, and this species appears to have a single origin (17).

**Can the genomic composition of the ancient hybrid species be predicted from QTL analyses of synthetic hybrids?** The experiments described above show that hybridization could have facilitated ecological divergence, but do not prove that it actually did so. An alternative hypothesis, for example, is that the ecological differences that characterize the three ancient hybrid species arose through mutational divergence and were incidental to hybrid origin. To determine whether hybridization

actually did facilitate ecological divergence, we compared the genomic composition of the three ancient hybrid species with predictions from the QTL analyses of the BC<sub>2</sub> population of *H. annuus* × *H. petiolaris*.

To estimate genomic composition, we generated high-resolution genetic linkage maps, based primarily on microsatellite and amplified fragment length polymorphism (AFLP) markers (21), for each of the three ancient hybrid species. Seventeen linkage

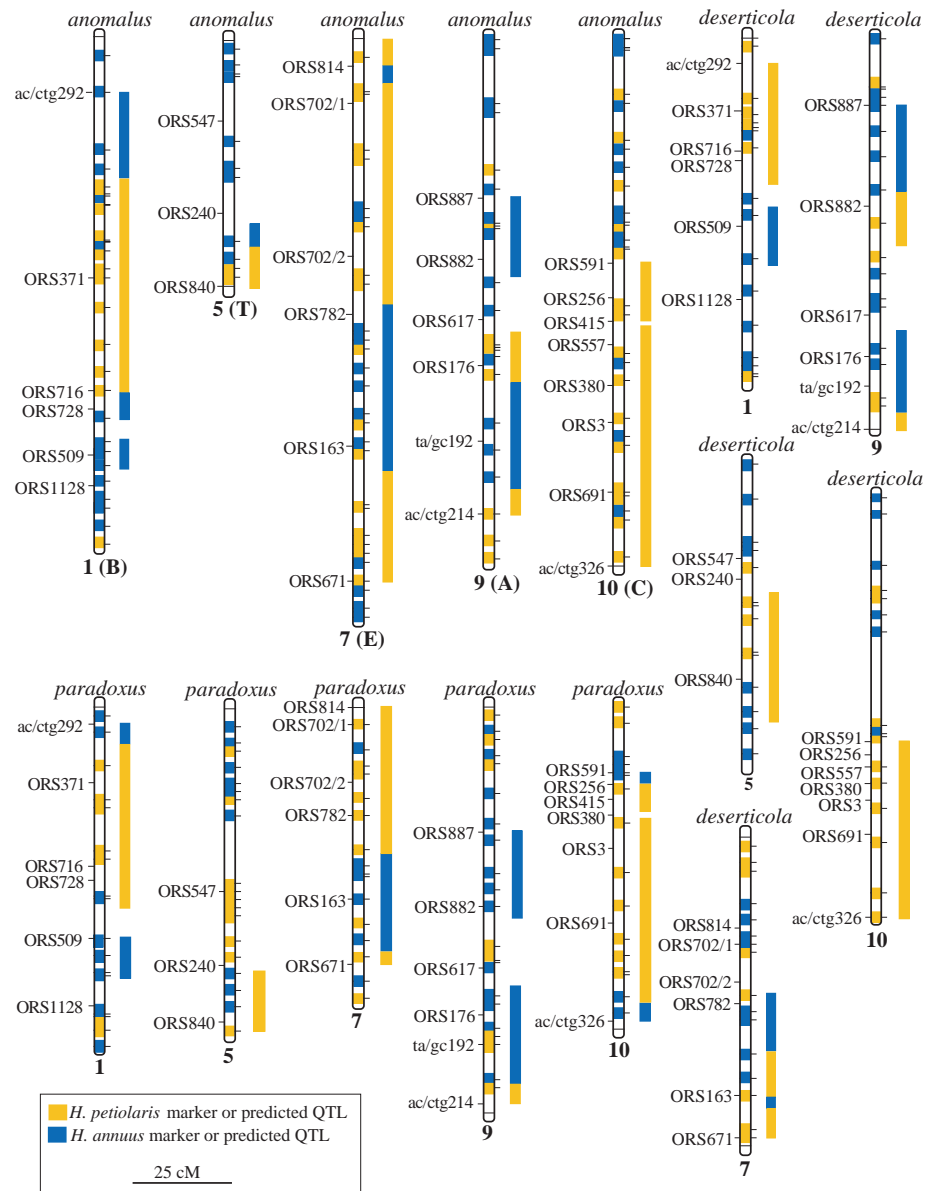


**Fig. 2.** Comparison of the genomic composition of the ancient hybrid species with predictions from the QTL analyses (Fig. 1) (fig. S1) for five collinear chromosomes (see fig. S2 for the remaining 12 chromosomes). Linkage groups are designated by number according to the standard nomenclature for sunflower (27). Letter(s) in parentheses after linkage group designations for *H. anomalus* enable comparisons with previous genetic mapping studies of this species (18, 30). Positions of molecular markers used in the QTL analyses are shown to the left of each linkage group, and the distribution of species-specific parental markers (table S4) is shown in the center of each linkage group, with markers derived from *H. annuus* in blue and those from *H. petiolaris* in yellow. Bars to the right of each linkage group indicate the parentage of chromosomal segments, as predicted from the QTL analyses.

## RESEARCH ARTICLES

groups were recovered for each of the three hybrid species, which corresponds to their haploid chromosome number (Fig. 2) (fig. S2). For *H. anomalus*, the present study added 318 markers to the previously published 701-marker map (30), bringing the total number of markers mapped to 1019. The 1019 markers spanned 1908.3 cM, with an average spacing between markers of 1.90 cM. The linkage maps for *H. deserticola* and *H. paradoxus* reported here comprise 672 and 771 markers, respectively. Map lengths and average marker spacing are 1229 cM and 1.88 cM, respectively, for *H. deserticola*, and 1420.5 cM and 1.88 cM, respectively, for *H. paradoxus*.

The most likely parental species origin of each mapped marker was then determined by surveying five natural populations each of *H. annuus* and *H. petiolaris* (21). In all, 427, 290, and 325 of the markers mapped in *H. anomalus*, *H. deserticola*, and *H. paradoxus*, respectively, could be assigned to one or the other parental species and thus were informative with respect to genomic composition (table S4).

We then used the  $\phi$  coefficient of association (21) to compare the genomic distribution of parental species markers in each of the ancient hybrids with predictions from the BC<sub>2</sub> QTL data. Species-specific parental markers mapped in each of the hybrid species either matched or did not match the identity of the predicted parental species donor for that genomic region (Fig. 2) (fig. S2).

Congruence between predicted and actual genomic composition was high (Fig. 2) (fig. S2), with  $\phi$  coefficient values of 0.56 ( $N = 150$ ,  $P < 0.001$ ) for *H. paradoxus*, 0.58 ( $N = 193$ ,  $P < 0.001$ ) for *H. anomalus*, and 0.65 ( $N = 94$ ,  $P < 0.001$ ) for *H. deserticola*. Because of limited map resolution for species-specific markers, we cannot determine the actual lengths of parental chromosomal segments. Possibly they are very large, as previously suggested for *H. anomalus* (30). If this were the case, it would suggest that hybrid speciation occurred rapidly, resulting in the fixation of large parental chromosomal segments that have remained largely intact since their initial establishment. Alternatively, the hybrid species' genomes may be considerably more fine-grained than shown here, and the clustering of markers derived from the same parental species may result from the preponderance of genetic material from that parent in a given genomic region (and not from the presence of a fully intact chromosomal segment). Either way, the ancient hybrid species appear to have the predicted combination of parental genetic material for producing their extreme phenotypes.

Previously (18), it was shown that three synthetic hybrid lineages of *H. annuus* ×

*H. petiolaris* converged onto a combination of chromosomal blocks that was similar to that found in *H. anomalus*, although some differences remained. The present data set accounts for aspects of the *H. anomalus* genotype that could not be explained by fertility selection alone. For many genomic regions, however, there was concordance between the predicted genomic composition from fertility selection and the QTL analysis of phenotypic differences, implying that genes causing hybrid inviability or sterility may overlap with those responsible for phenotypic differences.

**Conclusions.** Our results corroborate the view that hybridization can play an important creative role in adaptive evolution, and suggest a simple genetic mechanism (complementary gene action) by which this may occur. Whether these conclusions can be extrapolated to taxa other than *Helianthus* is less clear. Hybridization is frequent in many organismal groups (2), particularly plants (31), fish (32), and birds (33), and transgressive segregation appears to be the rule rather than the exception in interspecific crosses (22). Thus, an important and widespread role for hybridization in adaptive evolution is plausible. For hybridization to contribute to adaptation, however, fit hybrid genotypes must escape from "the mass of unfit recombinants" in a hybrid population [(7), although see (34)]. Mechanisms by which this may occur include asexual reproduction, selfing, diploid hybrid speciation (discussed herein), and the introgression of advantageous alleles (7). Unfortunately, little is known about the frequency of the latter two mechanisms, which are most applicable to sexual, outcrossing species.

Our results also suggest a largely unexplored mechanism for large and rapid adaptive transitions, such as the colonization of discrete and divergent ecological niches. Entry into discrete niches is theoretically difficult, because it may require simultaneous changes at multiple traits and/or genes. Hybridization offers a means by which this difficulty may be overcome because, unlike mutation, it provides genetic variation at hundreds or thousands of genes in a single generation. Moreover, new allelic variation introduced by hybridization has already been tested by selection in the genetic background of one of the parental species and thus is less likely to be deleterious.

Evolutionary biologists have struggled to link results from experimental microevolutionary studies of contemporary populations directly to evolutionary changes occurring in the distant past (34). Our results bridge this gap by showing that large morphological and ecological differences in three ancient hybrid sunflower species can be recreated through contemporary hybridization, and that these ancient hybrid spe-

cies have the predicted combination of parental chromosomal blocks for producing their phenotypes. Hence, hybridization did indeed facilitate major ecological transitions in wild sunflowers.

### References and Notes

1. E. Anderson, *Introgressive Hybridization* (Wiley, New York, 1949).
2. M. L. Arnold, *Natural Hybridization and Evolution* (Oxford Univ. Press, New York, 1997).
3. W. H. Wagner, *Taxon* **19**, 146 (1970).
4. E. Mayr, *Am. J. Bot.* **79**, 222 (1992).
5. D. W. Schemske, *Evolution* **54**, 1069 (2000).
6. J. F. Wendel, J. J. Doyle, in *Molecular Systematics of Plants II: DNA Sequencing*, D. E. Soltis, P. S. Soltis, J. J. Doyle, Eds. (Kluwer, Boston, 1998), pp. 265–296.
7. N. H. Barton, *Mol. Ecol.* **10**, 551 (2001).
8. V. Grant, *Plant Speciation* (Columbia Univ. Press, New York, 1981).
9. D. Greig, E. J. Louis, R. H. Borts, M. Travisano, *Science* **298**, 1773 (2002).
10. C. A. Buerkle, R. J. Morris, M. A. Asmussen, L. H. Rieseberg, *Heredity* **84**, 441 (2000).
11. E. M. McCarthy, M. A. Asmussen, W. W. Anderson, *Heredity* **74**, 502 (1995).
12. R. J. Abbott, *Trends Ecol. Evol.* **7**, 401 (1992).
13. L. H. Rieseberg, *Annu. Rev. Ecol. Syst.* **28**, 359 (1997).
14. L. H. Rieseberg, *Am. J. Bot.* **78**, 1218 (1991).
15. B. L. Gross, A. E. Schwarzbach, L. H. Rieseberg, *Am. J. Bot.*, in press.
16. A. E. Schwarzbach, L. H. Rieseberg, *Mol. Ecol.* **11**, 1703 (2002).
17. M. E. Welch, L. H. Rieseberg, *Evolution* **56**, 2126 (2002).
18. L. H. Rieseberg, B. Sinervo, C. R. Linder, M. Ungerer, D. M. Arias, *Science* **272**, 741 (1996).
19. L. H. Rieseberg, *Evolution* **54**, 859 (2000).
20. D. M. Rosenthal, A. E. Schwarzbach, L. A. Donovan, O. Raymond, L. H. Rieseberg, *Int. J. Plant Sci.* **162**, 387 (2002).
21. See supporting data on Science Online.
22. L. H. Rieseberg, M. A. Archer, R. K. Wayne, *Heredity* **83**, 363 (1999).
23. S. J. Gould, R. C. Lewontin, *Proc. R. Soc. London Ser. B* **205**, 581 (1979).
24. A. Danin, *J. Arid Environ.* **21**, 193 (1991).
25. A. C. Gibson, *Bioscience* **48**, 911 (1998).
26. C. Lexer, M. Welch, J. L. Durphy, L. H. Rieseberg, *Mol. Ecol.* **12**, 1225 (2003).
27. M. E. Welch, L. H. Rieseberg, *Am. J. Bot.* **89**, 472 (2002).
28. M. C. deVicente, S. D. Tanksley, *Genetics* **134**, 585 (1993).
29. R. R. Sokal, F. J. Rohlf, *Biometry* (Freeman, New York, ed. 3, 1995).
30. M. C. Ungerer, S. Baird, J. Pan, L. H. Rieseberg, *Proc. Natl. Acad. Sci. U.S.A.* **95**, 11757 (1998).
31. N. C. Ellstrand, R. Whitkus, L. H. Rieseberg, *Proc. Natl. Acad. Sci. U.S.A.* **93**, 5090 (1996).
32. C. L. Hubbs, *Syst. Zool.* **4**, 1 (1995).
33. P. R. Grant, B. R. Grant, *Science* **256**, 193 (1992).
34. P. R. Grant, B. R. Grant, *Science* **296**, 707 (2002).
35. Supported by NIH grant R01 G59065 and NSF grant DEB 9806290 (L.H.R.). We thank M.-J. Kim for assistance with genotyping, J. Lance for assistance with phenotyping, and S. Knapp for microsatellite primer sequences and mapping information.

### Supporting Online Material

www.sciencemag.org/cgi/content/full/1086949/DC1  
Materials and Methods  
Figs. S1 and S2  
Tables S1 to S4  
References

19 May 2003; accepted 10 July 2003  
Published online 7 August 2003;  
10.1126/science.1086949  
Include this information when citing this paper.